AIMS Mathematics, 10(12): 28470–28487.
DOI:10.3934/math.20251253
Received: 20 September 2025
Revised: 25 October 2025
Accepted: 11 November 2025
Published: 03 December 2025

https://www.aimspress.com/journal/Math

Research article

Nonuniform fast linear canonical transform based on low rank approximation

Yannan Sun* **and Jing Liu**

School of Mathematical Sciences, Jiangsu University, Zhenjiang 212013, Jiangsu, China

* **Correspondence:** Email: sunyannan@ujs.edu.cn.

Abstract: The investigations of the discrete and fast linear canonical transform (LCT) are becoming one of the hottest research topics in modern signal processing and optics. Among them, the fast calculation of LCT for nonuniform data is one of the key problems. In this paper, two novel fast algorithms based on low-rank approximation are presented. First, we propose two methods for approximate nonuniform time-domain sampling with uniform sampling. Second, we utilize a low rank matrix to approximate the nonuniform LCT kernel, combined with the exponential function and Taylor series. Then, the fast algorithms for nonuniform sampling in the time domain are developed, which cost K FFTs. Finally, we extend the fast algorithm to nonuniform LCT in the frequency and transform domains. The effectiveness of the proposed algorithm is verified by simulations.

Keywords: linear canonical transform; fast Fourier transform; Taylor series; approximation theory; nonuniform sampling
Mathematics Subject Classification: 11F20, 11M20

1. Introduction

Transforms are widely employed in signal processing to acquire useful information that is not explicitly available when the signal is in the time domain [1]. Most real-time signals, such as speech and biomedical signals, are non-stationary signals [2]. Many useful tools have been developed for processing these non-stationary signals [3–5]. Among them, the linear canonical transform (LCT), which describes the effect of quadratic phase systems on a wave field, is a parameterized general linear integral transform with three degrees of freedom. In optics, the LCT can describe a broad class of optical systems, including thin lenses, sections of free space in the Fresnel approximation, sections of quadratic graded-index media, and linear quadratic phase systems [6, 7]. The LCT generalizes many optical transforms, such as the Fourier transform and fractional Fourier transforms, coordinate scaling, chirp multiplication, and the Fresnel transform [8]. Compared with the zero parameter of the

Fourier transform, and one parameter of the fractional Fourier transform, the three free parameters of LCT let the nonband-limited signal in the traditional or fractional Fourier transform domain be a band-limited signal in the LCT domain under a certain condition. The LCT can be regarded as the affine transformation relationship in the time-frequency plane. The relationship not only includes the rotation relationship, but also includes compression and stretching and other relations, and the total support domain on the time frequency plane remains unchanged. These advantages make the LCT have a powerful role and potential in the field of signal processing. The LCT has also found many applications in the solution of optical systems, radar system analysis, filter design, pattern recognition, image watermarking, and many other fields [9]. Basic theories of LCT have been developed that include convolution theorems [10], sampling theorems [11], uncertainty principles [12], numerical calculations [8], and some extended research [13–15]. The numerical approximation of the LCT is important in the modeling of first-order optical systems and many signal processing applications.

Pei [16] firstly explored the discretization method of LCT and obtained the definition of the closed form of DLCT by sampling the time and the LCT domain at suitable intervals. A fast algorithm is obtained using the Chirp product and a fast Fourier transform (FFT). Subsequently, various fast algorithms for LCT have been proposed [17, 20, 22]. The existing discrete algorithms are divided mainly into the following categories. The first is that it decomposes an arbitrary LCT operator into its special cases that have a fast algorithm [18, 19, 26]. The second is eigenvector decomposition-type fast algorithms [24, 25], which is implemented by constructing the LCT kernel matrix using the spectral decomposition expression of the continuous LCT kernel function. The third is the DLCT-based algorithm [21, 23], which is similar to employing the FFT to implement the discrete Fourier transform. In addition to the above-mentioned algorithms, various other fast algorithms [27–29] have been presented. These research results provide a good basis for further development of the DLCT toward meeting the requirements of practical applications. Many aspects of the fast methods of the DLCT still need to be studied.

The aforementioned DLCT and its associated fast algorithms are developed exclusively under uniformly sampled conditions in both the time and the LCT domains. Nonuniform sampling is often encountered in practical applications, such as filter design, synthetic aperture radar (SAR) imaging, ultrasonic diffraction tomography, and magnetic resonance imaging (MRI). During SAR imaging, radar platform jitter or environmental noise interference often introduces perturbations in spatial sampling. In MRI, nonuniform frequency-domain sampling techniques are more suitable for rapid data acquisition and motion correction [30]. Direct calculation of the nonuniform DLCT requires $O(N^2)$ operations and cannot meet the needs of many practical applications. Therefore, it becomes necessary to study fast algorithms for nonuniform LCTs. In 2023, Sun and Qian developed the fast approximate algorithms of NUDLCT based on interpolation and oversampled FFT, which is called nonuniform fast LCT [30]. Since the algorithm performed an oversampled FFT, the complexity of the runtime and sampling was much higher than that of an N-point FFT. To address these problems, this paper proposes a new fast algorithm based on the Taylor series. Our central idea is to exploit a low-rank observation. We present two methods that approximate nonuniform sampling in the time domain to uniform sampling, which can transform the computation of nonuniform LCT into a uniform case. Combined with the properties of exponential functions and Taylor series, we convert the nonuniform LCT kernel matrix transform into a low rank matrix, which can reduce the computational complexity of nonuniform LCT. The two fast LCT algorithms are derived for different nonuniform sampling in

time domain, which can be implemented via K FFTs. The proposed method can be generalized to the computation of non-uniform LCT in the frequency domain, as well as in both the time and transform domains.

The two fast algorithms proposed in this paper can both reduce the computational complexity of non-uniform LCT from $O(N^2)$ to $O(KNlogN)$, while maintaining computational accuracy. However, these algorithms are designed for specific types of non-uniform sampling. For other types of non-uniformities, the algorithms may not perform efficiently.

The rest of this paper is organized as follows: The problems are described in Section 2. The main results are proposed in Section 3, and the algorithm complexities are analyzed under different nonuniform sampling. The simulations are presented to verify the effectiveness of the proposed algorithm in Section 4. Finally, this study is concluded in Section 5.

2. Description of the problems

The uniform discrete LCT (DLCT) of a discrete signal $f(n\Delta t)$, $n = 0, 1, \cdots, N-1$ is defined as [21]

$$F_m = \sum_{n=0}^{N-1} \sqrt{\beta} e^{-\frac{i\pi}{4}} f(n\Delta t) e^{i\pi\left[\alpha(m\Delta u)^2 - 2sgn(\beta)nm/N + \gamma(n\Delta u)^2\right]}, \tag{2.1}$$

where N is the length of the discrete signal, α, β, γ are LCT parameters, $0 \le m, n \le N-1$, and Δt and Δu are the sampling intervals in the time and LCT domains. It can be calculated by fast discrete linear canonical transform(FDLCT) [16, 18–21, 23]. When the sampling interval is non-uniform, Eq (2.1) becomes a nonuniform discrete linear canonical transform (NUDLCT),

$$H_m = \sum_{n=0}^{N-1} f(t_n) \sqrt{\beta} e^{\frac{i\pi}{4}} e^{i\pi[\alpha u_m^2 - 2\beta u_m t_n + \gamma t_n^2]}, \tag{2.2}$$

where $0 \le m \le N-1, t_0, t_1, \cdots, t_{N-1} \in [0, 1/|\beta|\Delta u]$ is the sampling in the time domain, and $u_0, u_1, \cdots, u_{N-1} \in [0, N\Delta u]$ is the sampling in the LCT domain. Computing Eq (2.2) directly costs $2N(N-1)$ real additions and N^2 real multiplications. If the samplings are equispaced namely, $u_m = m\Delta u, t_n = n\Delta t$, $(\Delta u \cdot \Delta t = 1/(N|\beta|))$, then the transform is fully uniform and Eq (2.2) can be computed by the FDLCT in $O(N \log N)$ operations. Unfortunately, the FDLCT is not useful when either the samples are non-equispaced or the frequencies are non-integer. The NUDLCT has the following three types:

(1) Nonuniform sampling in the time domain but uniform in the LCT domain: in Eq (2.2), the variable u in the LCT domain is discretized uniformly at N points with sampling intervals Δu, whereas the sample point $t_0, t_1, \cdots, t_{N-1}$ in the time domain is nonuniform in $[0, 1/|\beta|\Delta u]$. This corresponds to evaluating a generalized LCT series at equispaced points. In Section 3.1, we describe a quasi-optimal algorithm, referred to as nonuniform fast linear canonical transform(NUFDLCT-I). In section 3.2, we derive a fast algorithm when the sampling is arbitrary, referred to as nonuniform fast linear canonical transform(NUFDLCT-II).

(2) Uniform sampling in the time domain but nonuniform sampling in the LCT domain: in Eq (2.2), $t_n = n\Delta u$ and the LCT domain is non-uniform. This NUDLCT corresponds to evaluating a linear

canonical series at nonequispaced points. In Section 3.3, we derive an algorithm for computing the this NUDLCT by combining our NUFDLCT-I.

(3) Nonuniform sampling in both time and LCT domains: in Eq (2.2), the samples $t_0, t_1, \cdots, t_{N-1}$ are nonuniform in the time domain and the samples $u_0, u_1, \cdots, u_{N-1}$ are also nonuniform in LCT domain. This is fully nonuniform transform and corresponds to evaluating a generalized linear canonical series at non-equispaced points. In Section 3.3, we present a fast algorithm for computing this NUDLCT by combining our NUFDLCT-II.

For the above three cases, we focus on the fast algorithms for the first case, namely:

$$F_m = \sum_{n=0}^{N-1} f(t_n)\sqrt{\beta}e^{\frac{i\pi}{4}}e^{i\pi[\alpha(m\Delta u)^2-2\beta m\Delta u t_n+\gamma t_n^2]}, \tag{2.3}$$

where $0 \le m \le N-1$. The other two cases are realized by the relationship between the discrete transformation kernel matrix.

For different nonuniform sampling, combining with the approximation principle and the nature of the discrete LCT, the kernel matrix is approximated as a low-rank matrix, and the two kinds of fast algorithms for Eq (2.3)'s non-uniformity are proposed in the following section.

3. Main results

The algorithms presented in this paper are based on a simple observation: when the samplings are near-equispaced, then $\tilde{F}_1 \oslash F$ can be well-approximated by a low-rank matrix [31]. That is, for a small integer K, we find that,

$$\tilde{F}_1 \oslash F \approx \underline{v}_0\underline{w}_0^T + \underline{v}_1\underline{w}_1^T + \cdots + \underline{v}_{K-1}\underline{w}_{K-1}^T, \tag{3.1}$$

where $\underline{v}_0, \underline{v}_1, \cdots, \underline{v}_{K-1}, \underline{w}_0, \underline{w}_2, \cdots, \underline{w}_{K-1} \in \mathbb{C}^{N\times 1}$,

$$(F)_{mn} = e^{-2\pi imn/N}, (\tilde{F}_1)_{mn} = e^{-2\pi i\beta m\Delta u t_n},$$

$\oslash$ denotes the Hadamard division; that is, $C = A \oslash B$ means that $(C)_{mn} = (A \oslash B)_{mn} = A_{mn}/B_{mn}$.

In this section, we consider how to approximate the kernel matrix of Eq (2.3) as a low-rank matrix to achieve fast computation, where the time-domain sampling points are quasi-uniform and random, respectively.

3.1. The first type of fast algorithm for nonuniform linear canonical transform

3.1.1. Algorithm derivation

Assumed that the samplings $t_0, t_1, \cdots, t_{N-1}$ are quasi-uniform sampling and satisfy

$$|t_n - \frac{n}{N|\beta|\Delta u}| \le \frac{\theta}{N|\beta|\Delta u}, \tag{3.2}$$

where $0 \le n \le N-1; 0 \le \theta \le 1/2$. This assumption guarantees that $n/(N|\beta|\Delta u)$ is the closest equispaced point to t_n, which simplifies the description of our algorithm. Using the properties of exponential functions, we obtain the following Theorem 1.

Theorem 1. *Let the nonuniform LCT of the discrete signal $f(t_k)$ be Eq (2.3) for $k = 0, 1, 2, \cdots, N-1$. If the discrete sampling $t_0, t_1, \cdots, t_{N-1}$ satisfies Eq (3.2), the Eq (2.3) can be factored, as*

$$\underline{f} \approx D \sum_{r=0}^{K-1} D_{\underline{v}_r} F D_{\underline{w}_r} \underline{c}, \tag{3.3}$$

where $0 \le m, n \le N-1$, $(F)_{mn} = e^{-2\pi i m \frac{n}{N}}$

$$\underline{c} = (f(t_0)\sqrt{\beta}e^{-\frac{i\pi}{4}+i\pi\gamma t_0^2}, f(t_1)\sqrt{\beta}e^{-\frac{i\pi}{4}+i\pi\gamma t_1^2}, \cdots, f(t_{N-1})\sqrt{\beta}e^{-\frac{i\pi}{4}+i\pi\gamma t_{N-1}^2}),$$

$$D = diag(1, e^{i\pi\alpha(\Delta u)^2}, \cdots, e^{i\pi\alpha((N-1)\Delta u)^2}),$$

$$\underline{v}_r = (N(\underline{t} - \underline{e}))^r, \underline{w}_r = (-i\beta)^r (2\pi\underline{\omega}/N)^r / r!,$$

$$D_{\underline{v}_r} = diag((Nt_0)^r, (N(t_1 - \frac{1}{N|\beta|\Delta u}))^r, \cdots, (N(t_{N-1} - \frac{N-1}{N|\beta|\Delta u}))^r), \tag{3.4}$$

$$D_{\underline{w}_r} = diag(0, \frac{(-2\pi i\beta\Delta u)^r}{N^r r!}, \cdots, \frac{(-2\pi i\beta(N-1)\Delta u)^r}{N^r r!}). \tag{3.5}$$

Proof. First, we convert Eq (2.3) as,

$$\underline{f} = D\tilde{F}_1 \underline{c}, (\tilde{F}_1)_{mn} = e^{-2\pi i\beta m\Delta u t_n}, \tag{3.6}$$

where

$$\underline{c} = (f(t_0)\sqrt{\beta}e^{-\frac{i\pi}{4}+i\pi\gamma t_0^2}, f(t_1)\sqrt{\beta}e^{-\frac{i\pi}{4}+i\pi\gamma t_1^2}, \cdots, f(t_{N-1})\sqrt{\beta}e^{-\frac{i\pi}{4}+i\pi\gamma t_{N-1}^2}),$$

$$D = diag(1, e^{i\pi\alpha(\Delta u)^2}, \cdots, e^{i\pi\alpha((N-1)\Delta u)^2}),$$

$$\underline{f} = [\underline{f}(0), \underline{f}(1), \cdots, \underline{f}(N-1)]^T.$$

Using the properties of the exponential function, the matrix $\tilde{F}_1$ is decomposed as

$$\tilde{F}_1 = A \circ F, \tag{3.7}$$

where $\circ$ is Hadamard product, the element of the matrix A is

$$A_{mn} = e^{-2\pi i\beta m\Delta u(t_n - \frac{n}{N|\beta|\Delta u})}, 0 \le m, n \le N-1.$$

Combining Eq (3.7), the Eq (3.6) can be written as:

$$\underline{f} = D(A \circ F)\underline{c}. \tag{3.8}$$

In this section, consider the Taylor expansion of $e^{-x} = 1 - x + x^2/2 - x^3/6 + \cdots$ for $x = 0$. Applying this Taylor series to each entry of the matrix A, we find that for $0 \le m, n \le N-1$

$$A_{mn} = e^{-2\pi i\beta m\Delta u(t_n - \frac{n}{N|\beta|\Delta u})} = \sum_{r=0}^{\infty} \frac{(-2\pi i\beta(t_n - \frac{n}{N|\beta|\Delta u})m\Delta u)^r}{r!}, \tag{3.9}$$

where the expansion is truncated after K terms to be regarded as an approximation,

$$A_{mn} \approx \sum_{r=0}^{K-1} \frac{(-2\pi i\beta(t_n - \frac{n}{N|\beta|\Delta u})m\Delta u)^r}{r!}. \tag{3.10}$$

Now, we assume $\underline{t} = (t_0, t_1, \cdots, t_{N-1})^T$, $\underline{e} = (0, \frac{1}{N|\beta|\Delta y}, \cdots, \frac{N-1}{N|\beta|\Delta u})^T$, $\omega = (0, \Delta u, \cdots, (N-1)\Delta u)^T$, the Eq (3.9) can be applied to each entry of A to find that

$$\begin{aligned} A = e^{-2\pi i\beta((\underline{t}-\underline{e})\omega^T)} &\approx \sum_{r=0}^{K-1} \frac{(-i\beta)^r}{r!}(2\pi\omega^T(\underline{t}-\underline{e}))^r \\ &= \underline{v}_0\underline{w}_0^T + \underline{v}_1\underline{w}_1^T + \cdots + \underline{v}_{K-1}\underline{w}_{K-1}^T = A_K, \end{aligned} \tag{3.11}$$

where

$$\underline{v}_r = (N(\underline{t}-\underline{e}))^r, \underline{w}_r = (-i\beta)^r(2\pi\underline{w}/N)^r/r!, r = 0, 1, \cdots K-1.$$

Combining Eqs (3.6) and (3.11), we have

$$\underline{f} = D(A \circ F)\underline{c} \approx D(\sum_{r=0}^{K-1} \underline{v}_r\underline{w}_r^T \circ F)\underline{c}, \tag{3.12}$$

We convert the Eq (3.12) into matrix form,

$$\underline{f} \approx D\sum_{r=0}^{K-1} D_{\underline{v}_r} F D_{\underline{w}_r}\underline{c}, \tag{3.13}$$

where $D_{\underline{v}_r}$ and $D_{\underline{w}_r}$ are defined as Eqs (3.4) and (3.5).

Theorem 1 has been proven. □

Since $|-2\pi i\beta(t_n - \frac{n}{N|\beta|\Delta u})m\Delta u| \le 2\pi\theta$, the truncation error of the Taylor series of A is $\|A - A_K\| \le \varepsilon$ and $K = O(\log(1/\varepsilon))$ [32]. An approximation to $D\tilde{F}_1\underline{c}$ can be computed in $O(KN\log N)$ operations via the FFT, as each term in the sum in Eq (3.13) involves diagonal matrices and the DFT matrix. Moreover, each matrix-vector product in the sum can be computed independently, and the resulting vectors added together. This algorithm is referred to as NUFDLCT-I. In the next section, we will present a computational complexity analysis of the NUFDLCT-I.

3.1.2. Complexity analysis

Table 1 presents the computations of the algorithm. The computational complexity of the algorithm is determined by the length of the input signal N and the term of Taylor series expansion terms K. A computational comparison between NUFDLCT-I and the direct method is illustrated in Figure 1 when N = 512. Figure 1(a) shows real multiplication computation NUFDLCT-I and NUDLCT; Figure 1(b) shows the savings in real multiplication computation. The results show that the more sampling points, the more effective the NUFDLCT-I computation is.

Table 1. Computational analysis of NUFDLCT-I.

	Real multiplications	Real additions
NUDLCT	$4N^2$	$2N(2N-1)$
NUFDLCT-I	$2KN\log N$	$3KN\log N + 2KN$
Computation saving	$4N^2 - 2KN\log N - 2KN$	$2N(2N-1) - 3KN\log N - 2KN$

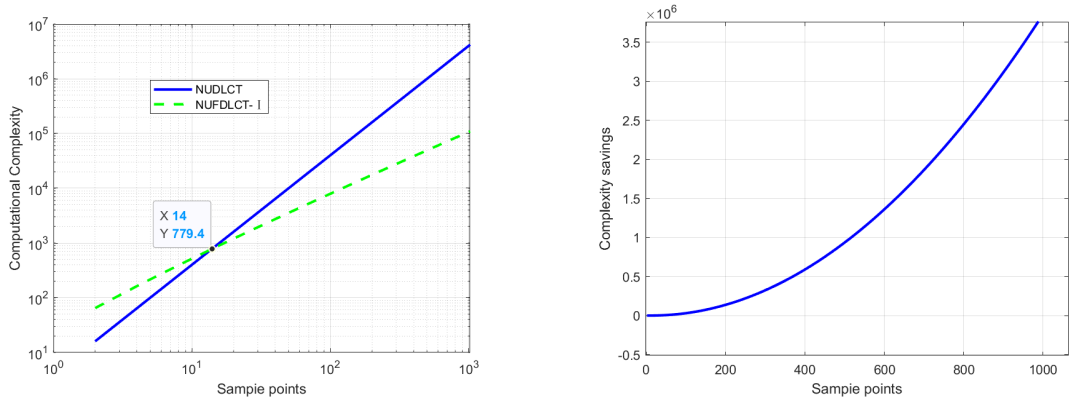

(a) (b)

Figure 1. Comparison of NUFDLCT-I and NUDLCT computations: (a) Calculation of NUDLCT and NUFDLCT-I; (b) Saving in calculations.

The algorithm reduces the computational cost from $2N(2N-1)$ real number additions to $3KN\log N + 2KN$ real number additions. Figure 1 shows that the computational savings increase with N. This confirms that the effectiveness of our method improves with the number of sample points N.

Assuming that the sampling $\underline{t} = (t_0, t_1, \cdots, t_{N-1})^T$ in Eq (2.3) is arbitrarily distributed, which makes the NUFDLCT-I no longer valid. Therefore, for this case, the other fast algorithm for Eq (2.3) will be given in this section, referred to as the second type of fast algorithm for nonuniform linear canonical transform (NUFDLCT-II).

3.2. The second type of fast algorithm for nonuniform linear canonical transform

Since $t \to e^{-2\pi i\beta m\Delta ut}$, $0 \le m \le N-1$ is periodic with a period of $1/|\beta|\Delta u$, for convenience, in this section, we assume $t_0, t_1, \cdots, t_{N-1} \in [0, 1/|\beta|\Delta u]$. Otherwise, we can translate to that interval using periodicity.

Defining a sequence $s_0, s_1, \cdots, s_{N-1} \in \{0, 1, \cdots, N-1\}$ and is defined so that $s_n/N|\beta|\Delta u$ is the closest point of t_n, since each t_n is spaced at a maximum distance of $1/2N|\beta|\Delta u$ from these equidistant points, we have

$$|t_n - \frac{s_n}{N|\beta|\Delta u}| \le \frac{1}{2N|\beta|\Delta u}, 0 \le n \le N-1. \tag{3.14}$$

The Eq (3.14) shows that nonuniform sampled points on are allocated to the nearest equidistant points. Figure 2 illustrates this process when $N = 10$. The sequence $s_0, s_1, \cdots, s_{N-1}$ can be calculated using $\underline{s} = round(N|\beta|\Delta u\underline{t})$, where $round(\star)$ is the integer closest to $\star$. In this case, the sequence

$s_0, s_1, \cdots, s_{N-1}$ take the values $s_0 = s_1 = 0, s_2 = 1, s_3 = 2, s_4 = 3, s_5 = s_6 = 5, s_7 = 7, s_8 = 8, s_9 = 10$, where $0 \le t_0 \le t_1 \le \cdots \le t_{N-1} < 1/|\beta|\Delta u$, but the ordering of the sample is not essential.

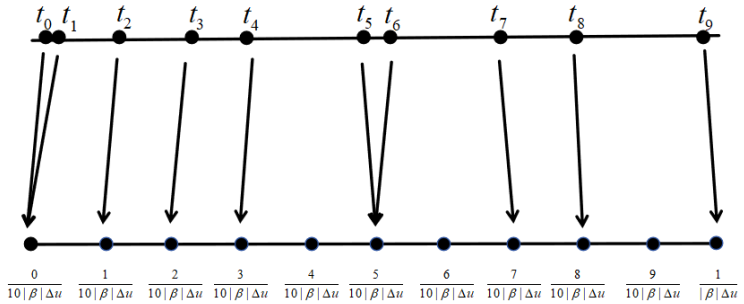

Figure 2. The nonuniform sample on $[0, 1/|\beta|\Delta u]$ to the nearest equidistant point when $N = 10$.

Exploiting the periodicity of the complex exponential, t_n is assigned to equally spaced nodes at 0 by

$$e^{-2\pi i\beta m\Delta u s_n/N|\beta|\Delta u} = e^{-2\pi i m s_n/N} = e^{-2\pi i m 0/N} = 1.$$

Defining the sequence $\underline{x} = (x_0, x_1, \cdots, x_{N-1})^T, x_k \in \{0, 1, \cdots, N-1\}, k = 0, 1, \cdots N-1$ to satisfy

$$x_n = \begin{cases} s_n, & 0 \le s_n \le N-1 \\ 0, & s_n = N \end{cases}. \tag{3.15}$$

We utilize these characteristics and combine them with Taylor series to propose the second fast algorithm for nonuniform LCT, which is derived as the following theorem.

Theorem 2. *Let the nonuniform LCT of the discrete signal $f(t_k), k = 0, 1, 2, \cdots, N-1$ be Eq (2.3). The discrete sampling $t_0, t_1, \cdots, t_{N-1}$ satisfies Eq (3.14); we can obtain an approximation $\underline{f}$ for f, as*

$$\underline{f} \approx D \sum_{r=0}^{K-1} D_{\underline{z}_r} F(:, \underline{x}) D_{\underline{w}_r} \underline{c}, \tag{3.16}$$

where $0 \le m, n \le N-1, r = 0, 1, 2, \cdots, K-1$,

$$\left(F(:, \underline{x})\right)_{mn} = e^{-2\pi i x_n m/N},$$

$$\underline{z}_r = (N(\underline{t} - \frac{\underline{s}}{N|\beta|\Delta u}))^r,$$

$$D_{\underline{z}_r} = diag((N(t_0 - \frac{s_0}{N|\beta|\Delta u}))^r, (N(t_1 - \frac{s_1}{N|\beta|\Delta u}))^r, \cdots, (N(t_{N-1} - \frac{s_{N-1}}{N|\beta|\Delta u}))^r).$$

Proof. Using the characteristic of the indices and the definition of $x_k (k = 0, 1, \cdots, N-1)$, the matrix $\tilde{F}_1$ in Eq (3.6) is decomposed as

$$\tilde{F}_1 = B \circ F(:, \underline{x}), \tag{3.17}$$

where the elements of matrix B and $F(:, \underline{x})$ are respectively,

$$(B)_{mn} = B_{mn} = e^{-2\pi i\beta(t_n - s_n/N|\beta|\Delta u)m\Delta u},$$

$$\left(F(:,\underline{x})\right)_{mn} = e^{-2\pi i x_n m/N}, 0 \le m, n \le N-1,$$

$\underline{x} = (x_0, x_1, \cdots, x_{N-1})$. Note that $F(:,\underline{x})$ represents the matrix formed by extracting the columns indexed by $(x_0, x_1, \cdots, x_{N-1})$ from the DFT matrix

This means that the (m,n) entry of $\tilde{F}_1$ can be expressed as a product of $e^{-2\pi i\beta(t_n - s_n/N|\beta|\Delta u)m\Delta u}$ and the (x_n, m) entry of F for $0 \le m, n \le N-1$. Expanding each element in the matrix B using the Taylor series yields

$$B_{mn} = e^{-2\pi i\beta(t_n - s_n/N|\beta|\Delta u)m\Delta u} = \sum_{r=0}^{\infty} \frac{(-2\pi i\beta(t_n - \frac{s_n}{N|\beta|\Delta u})m\Delta u)^r}{r!}, \tag{3.18}$$

Since $N(t_n - s_n/N \mid \beta \mid \Delta u)\beta\Delta u \in [-1/2, 1/2], m/N \in [0,1]$, we choose a suitable integer K such that $\|B - B_K\| \le \varepsilon$. Therefore, by extracting the first K items in Eq (3.18), we obtain

$$B_{mn} \approx \sum_{r=0}^{K-1} \frac{(-2\pi i\beta(t_n - \frac{s_n}{N|\beta|\Delta u})m\Delta u)^r}{r!}, \tag{3.19}$$

then the matrix B can be approximated as B_k

$$\begin{aligned} B = e^{-2\pi i\beta\omega^{\mathrm{T}}(\underline{t} - \frac{\underline{s}}{N|\beta|\Delta u})} \approx B_K &= \sum_{r=0}^{K-1} \frac{(-i\beta)^r}{r!}(2\pi\omega^{\mathrm{T}}(\underline{t} - \frac{\underline{s}}{N \mid \beta \mid \Delta u}))^r \\ &= \sum_{r=0}^{K-1} \underline{z}_r \underline{w}_r^T, \end{aligned} \tag{3.20}$$

where $\underline{w}_r^T$ and $\underline{t}$ are the same as Theorem 1, $\underline{s} = (s_0, \cdots, s_{N-1})^T$,

$$\underline{z}_r = (N(\underline{t} - \frac{\underline{s}}{N|\beta|\Delta u}))^r,$$

Thus, Eq (2.3) can be approximately calculated as:

$$\underline{f} = D\tilde{F}_1\underline{c} = D(B \circ F(:,\underline{x}))\underline{c} \approx D(B_K \circ F(:\underline{x}))\underline{c} = D\sum_{r=0}^{K-1} D_{\underline{z}_r} F(:\underline{x}) D_{\underline{w}_r}\underline{c}, \tag{3.21}$$

where

$$D_{\underline{z}_r} = diag((N(t_0 - \frac{s_0}{N|\beta|\Delta u}))^r, (N(t_1 - \frac{s_1}{N|\beta|\Delta u}))^r, \cdots, (N(t_{N-1} - \frac{s_{N-1}}{N|\beta|\Delta u}))^r).$$

Theorem 2 has been completed. □

The matrix-vector products with the diagonal matrices $D_{\underline{\omega}_r}$, D, and $D_{\underline{z}_r}$ can be performed in $O(N)$ operations, and $F(:\underline{x})\underline{c}$ can be calculated in $O(N\log N)$ operations via the FFT. In addition, each term in the sum in Eq (3.16) can be calculated in parallel, and the resulting vectors added together afterwards. This algorithm is the second kind of fast algorithm for nonuniform linear canonical transforms (NUFDLCT-II). The analysis shows that the computation of NUFDLCT-II is the same as that of NUFDLCT-I.

In this section, we mainly derive the two fast algorithms with non-uniform sampling in the time domain but uniform sampling in the transform domain for different sampling situations. We found that the two algorithms are based on approximation theory, combined with Taylor expansion to decompose the discrete transform kernel matrix into the sum of low-rank matrices, and use FFT to achieve fast calculation. For the other two nonuniform LCT fast algorithms, the relationship between the three discrete transform kernel matrices is analyzed, and the corresponding fast algorithm is proposed in the next section.

3.3. Fast algorithms for nonuniform LCT in two other cases

When the time domain is uniform sampling and the LCT domain is non-uniform, the LCT of the discrete signal $f(n\Delta t)$ is defined as

$$\begin{aligned} \underline{g}(m) &= \sqrt{\beta}e^{-i\pi/4}e^{i\pi\alpha u_m^2}\sum_{n=0}^{N-1} f(n\Delta u)e^{-2\pi i\beta n\Delta t u_m}e^{i\pi\gamma(n\Delta t)^2} \\ &= \sqrt{\beta}e^{-i\pi/4}e^{i\pi\alpha u_m^2}\sum_{n=0}^{N-1} f(n\Delta u)(\tilde{F}_2)_{mn}e^{i\pi\gamma(n\Delta t)^2}, \end{aligned} \tag{3.22}$$

where $(\tilde{F}_2)_{mn} = e^{-2\pi i\beta n\Delta t u_m}$, $u_0, u_1, \cdots, u_{N-1} \in [0, N]$ are sampling in the LCT domain.

It can be found that

$$(\tilde{F}_2)_{mn} = e^{-2\pi i\beta n\Delta t u_m} = e^{-2\pi i\beta\Delta t u_m n} = (\tilde{F}_1)_{nm}, 0 \le m, n \le N-1, \tag{3.23}$$

where $\Delta tu_0, \Delta tu_1, \cdots, \Delta tu_{N-1}$ serves as the nonuniform sampling of NUDLCT-I. It can be seen that matrix $\tilde{F}_2$ is the transpose of matrix $\tilde{F}_1$, and is possible to obtain

$$\underline{g}(m) = D\underline{F_2}\underline{C} = D(A \circ F)^T\underline{C} \approx D(A_K \circ F)^T\underline{C} = D\sum_{r=0}^{K-1} D_{\underline{w_r}}F^T D_{\underline{v_r}}\underline{C}, \tag{3.24}$$

Therefore, the fast algorithms for Eq (3.22) can be realized by NUFDLCT-I.

When the time domain and the LCT domain are nonuniform, the nonuniform LCT of $f(t_n)$ is defined as Eq (2.2), and can also be expressed

$$\underline{h}(m) = \sqrt{\beta}e^{-\frac{i\pi}{4}}\sum_{n=0}^{N-1} f(t_n)(\tilde{F}_3)_{mn}e^{i\pi\gamma t_n^2}, \tag{3.25}$$

where $(\tilde{F}_3)_{mn} = e^{-2\pi i\beta t_n u_m}$, $0 \le n, m \le N-1$.

By the nature of the exponential function, the matrix $\tilde{F}_3$ can be decomposed as:

$$(\tilde{F}_3)_{mn} = e^{-2\pi i\beta u_m(t_n - s_n/N|\beta|\Delta u)}e^{-2\pi i\beta u_m((s_n - x_n)/N|\beta|\Delta u)}\underbrace{e^{-2\pi i\beta u_m(x_n/N|\beta|\Delta u)}}_{\tilde{F}_2(:,\underline{x})}, \tag{3.26}$$

Equation (3.26) is represented as the following matrix form

$$\tilde{F}_3 = C \circ G \circ \tilde{F}_2(:, \underline{x}), \tag{3.27}$$

where

$$C_{mn} = e^{2\pi i\beta(t_n - s_n/N|\beta|\Delta u)u_m}, G_{mn} = e^{-2\pi i\beta((s_n - x_n)/N|\beta|\Delta u)u_m},$$
$$(\tilde{F}_2(:, \underline{x}))_{mn} = e^{-2\pi i\beta u_m(x_n/N|\beta|\Delta u)},$$

when $0 \le m, n \le N-1$, the $|N\beta\Delta u(t_n - s_n/N|\beta|\Delta u)| \le 1/2$ and $u_m/N\Delta u \in [0, 1)$ are satisfied.

Taylor expansion of the matrix C yields an approximation matrix of rank K. Furthermore, the rank of the matrix G is at most equal to 2, because

$$M = (\mathbf{1} - (\underline{s} - \underline{x})/N)\mathbf{1}^T + ((\underline{s} - \underline{x})/N)e^{-2\pi i\beta\underline{u}^T/|\beta|\Delta u}, \tag{3.28}$$

where $\mathbf{1}$ is a dimension column vector with element 1. $\underline{s} = (s_0, s_1, \cdots, s_{N-1})^T$, $\underline{x} = (x_0, x_1, \cdots, x_{N-1})$, $\underline{u} = (u_0, u_1, \cdots, u_{N-1})^T$. Since $C \circ G$ can be well represented by a rank matrix $O(K)$, fast algorithms can be implemented for this case using NUFDLCT-II.

4. Simulation

In order to prove the effectiveness of the proposed algorithms, simulations and comparisons with NUDLCT are given in this section. We consider the following linear FM signal

$$f(t_n) = \sum_{n=0}^{N-1}\sum_{j=1}^{M} A_j e^{-i\pi\lambda t_n^2 + ia_j t_n}, \tag{4.1}$$

where M is any positive integer, A_j is the amplitude, λ is the modulation frequency and a_j is the center frequency.

4.1. NUFDLCT-I simulations

To verify the effectiveness of the theory of NUFDLCT-I, we take the parameters in Eq (4.1) as

(i) $M = 1,\ A_1 = 1,\ \lambda = 3.5,\ a_1 = 10$;
(ii) $M = 3,\ A_1 = 2,\ A_2 = 5,\ A_3 = 10,\ \lambda = 8.5,\ a_1 = 4,\ a_2 = 8,\ a_3 = 6.5$.

For the signal (i), we take $\theta = 0.1$ and the transform parameters as $\alpha = 1.5$, $\beta = 2.5$, and $\gamma = 3.5$. The sampling points are $N = 512$, and the sampling interval is $\Delta u = 0.01$. We calculate the nonuniform DLCT of $f(t_n)$ using NUFDLCT-1 and directly NUDLCT. Figure 3 shows the errors between NUFDLCT-I and NUDLCT for $K = 6$ and $K = 8$. The results suggest that the computational accuracy of NUFDLCT-I and NUDLCT are similar, and the error decreases gradually as the value of K increases.

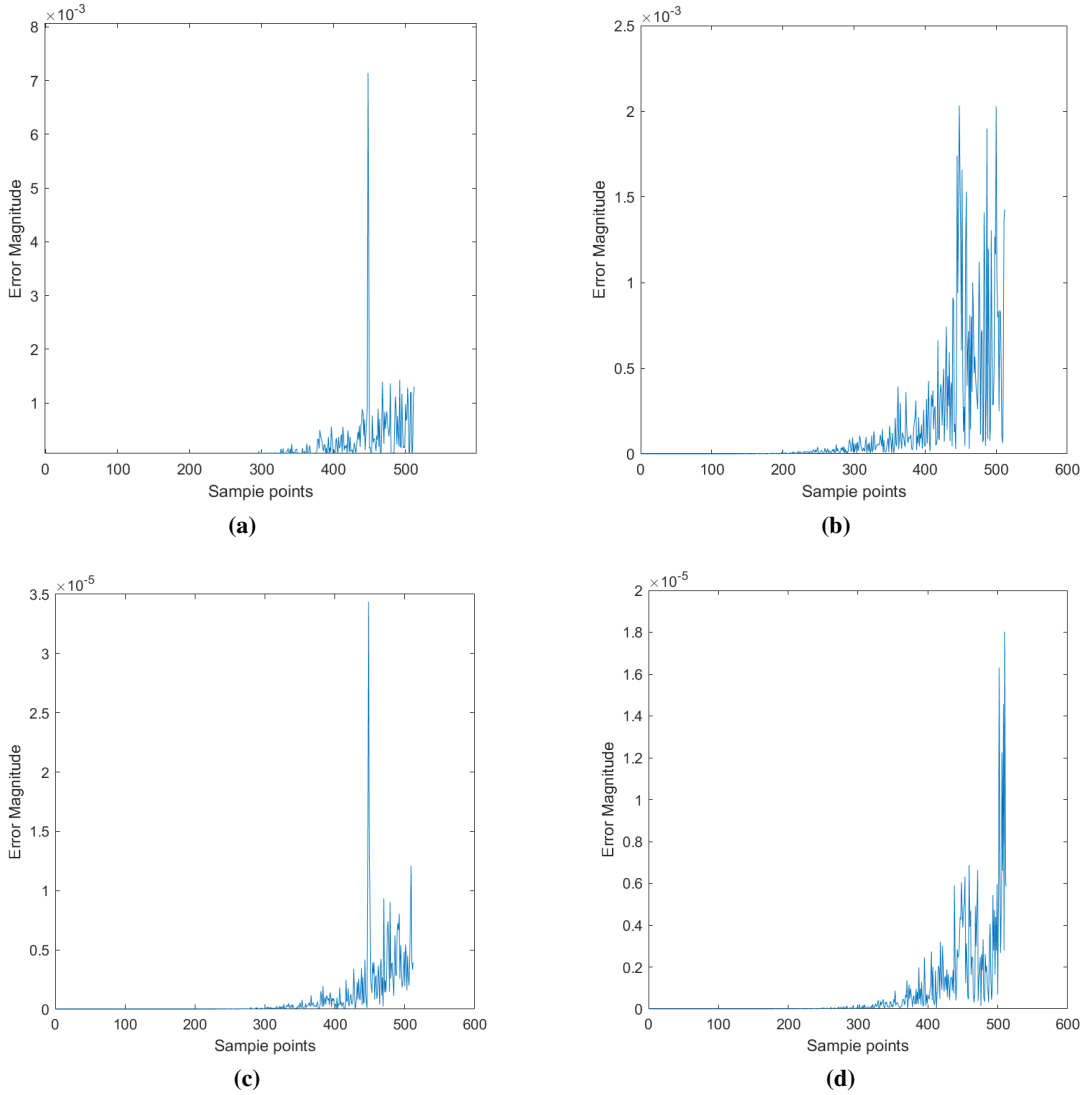

Figure 3. The real and imaginary errors between NUFDLCT-I and NUDLCT: (a) Real error for $K = 6$; (b) Imaginary error for $K = 6$; (c) Real error for $K = 8$; (d) Imaginary error for $K = 8$

Table 2 gives a comparison of computation results between NUFDLCT-I and NUDLCT in computing the LCT of the input signal when $K = 6$. The result shows that NUFDLCT-I has less computational than NUDLCT.

Table 2. Comparison of NUFDLCT-I and NUDLCT calculations.

	NUFDLCT-I	NUDLCT
Real multiplication	30720	262144
Real addition	39936	261632
Calculational savings of multiplication	231424	0
Calculational savings of addition	221696	0

The signal (ii) is multi-component chirp signal. We take $\theta = 0.1$, $N = 256$, the sampling interval are $\Delta u = 0.001$, and the LCT parameters $\alpha = 2.5$, $\beta = 3.5$, and $\gamma = 8.5$. Figure 4 gives the errors of the real and imaginary parts of the algorithm of NUFDLCT-I and directly NUDLCT, and the results show that the computational accuracy of NUFDLCT-I is similar to NUDLCT.

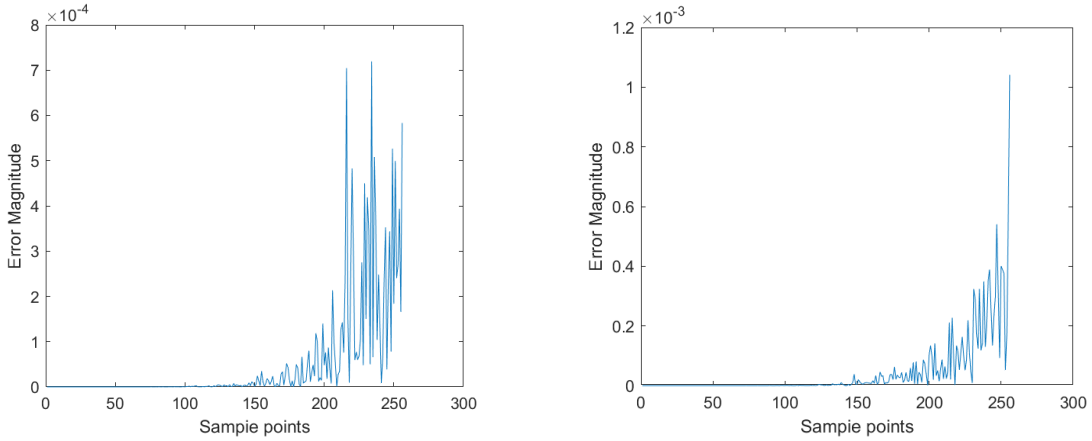

(a) **(b)**

Figure 4. Calculate the error of signal (ii) between NUFDLCT-I and NUDLCT: (a) Real error; (b) Imaginary error.

Table 3 gives the computation of NUFDLCT-I and NUDLCT in computing the LCT of the input signal when $K = 7$. The results indicate the superiority of NUFDLCT-I.

Table 3. Comparison of NUFDLCT-I and NUDLCT calculations.

	NUFDLCT-I	NUDLCT
Multiplication of real numbers	35840	262144
Addition of real numbers	46592	261632
Computational savings of multiplication	226304	0
Calculational savings of addition	215040	0

4.2. NUFDLCT-II simulations

We take $M = 1, A_1 = 3, \lambda = 2.5, a_1 = 6$, $N = 512, \Delta u = 0.01, \alpha = 1.5, \beta = 2.5, \theta = 0.1$ in Eq (4.1). The Figure 5 gives the errors of the real and imaginary between NUFDLCT-II and NUDLCT for $K = 14$, and the results also show that the computational accuracy of NUFDLCT-II and NUDLCT are similar.

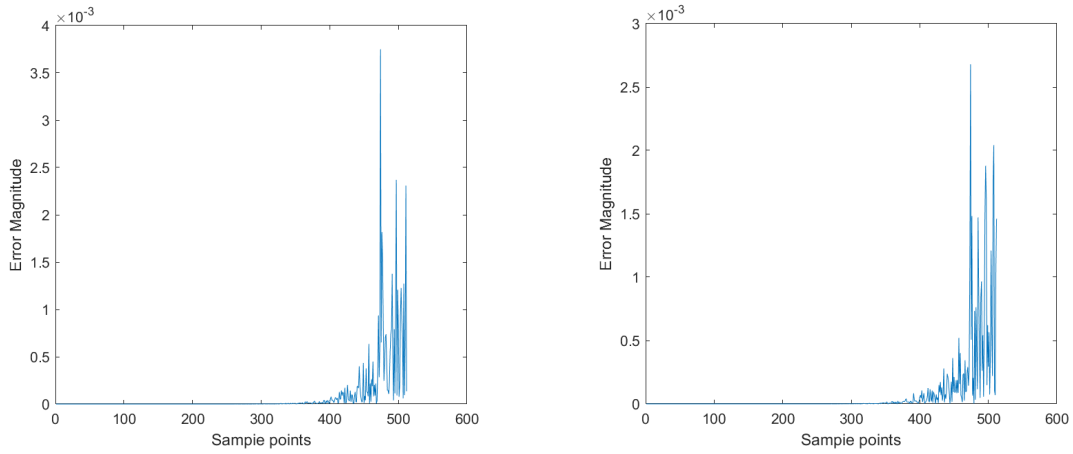

Figure 5. Calculate the error of signal (ii) between NUFDLCT-I and NUDLCT: (a) Real error; (b) Imaginary error.

Table 4 gives the computation of NUFDLCT-II and NUDLCT in calculating the LCT of the input signal when $K = 14$. The results show that NUFDLCT-II has smaller computation under guaranteed accuracy, and verifies the superiority of NUFDLCT-II when the samples are randomly sampled.

Table 4. Comparison of NUFDLCT-II and NUDLCT calculations.

	NUFDLCT-I	NUDLCT
Multiplicative calculus	71680	262144
Additive quantity	93184	261632
Calculations saved by multiplication	190464	0
Calculations saved by addition	168448	0

Figure 6 shows the computational complexity of NUFDLCT-II and NUDLCT under different signal lengths N. The results show that the longer the signal length is, the more effective NUFDLCT-II is.

The simulations presented above show that the theoretical results are consistent with practical applications. The proposed NUFDLCT-I and NUFDLCT-II provide a new tool for the computation of the nonuniform LCT.

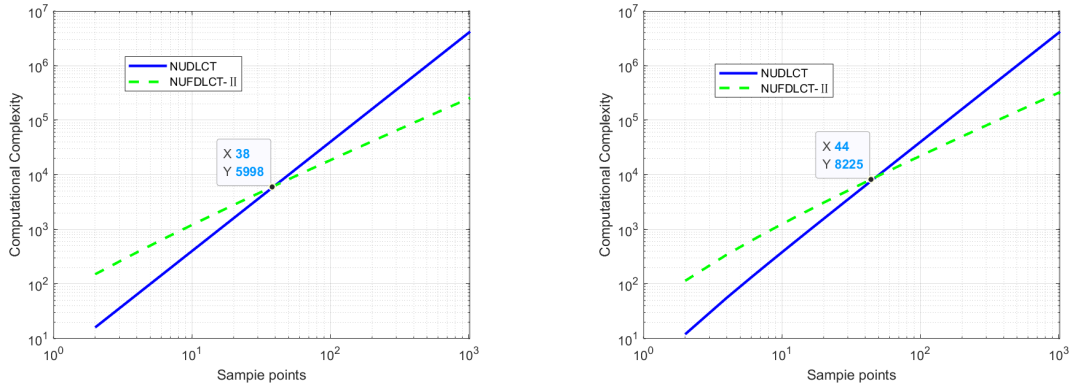

Figure 6. Computations of NUFDLCT-II and NUDLCT : (a) Real multiplication; (b) Real addition.

5. Conclusions

In this paper, we carry out related research on fast LCT algorithms for non-uniform data. In this process, sampling in the time domain is nonuniform and is uniform in the transform domain. The innovation of proposed algorithms can be summarized as

(1) For quasi-uniform sampling and arbitrary non-uniformity in time domain, NUFDLCT-I and NUFDLCT-II are proposed and are proposed based on approximation theory and Taylor series to transform the discrete LCT matrix into low-rank matrix.

(2) The framework of low-rank matrix approximation and K-stage FFT is introduced for the non-uniform linear canonical transformation, reducing complexity from $O(N^2)$ to $O(KNlogN)$.

(3) These fast algorithms extend to nonuniform LCT computation in frequency and transform domains, which can be implemented by K FFTs.

Numerical simulations show that the computational accuracy of the proposed algorithms continuously improves with an increasing number of Taylor series expansion terms, with low computational cost. The research results provide new research ideas for the study of fast algorithms for nonuniform LCTs.

Author contributions

Yannan Sun: Supervision, resources, conceptualization, funding acquisition, writing–review editing; Jing Liu: Formal analysis, methodology, writing–original draft, writing–review editing. All authors have read and agreed to the published version of the manuscript.

Use of Generative-AI tools declaration

The authors declare they have used Artificial Intelligence (AI) tools in the creation of this article.

Acknowledgments

The authors thank the editor and referees for their very helpful and detailed comments. This work is supported by the National Natural Science Foundation of China (No. 62001193).

Conflict of interest

The authors declare that there are no conflicts of interest regarding the publication of this paper.

References

1. H. E. Tahir, X. B. Zou, Z. H. Li, J. Y. Shi, X. D. Zhai, S. Wang, et al., Rapid prediction of phenolic compounds and antioxidant activity of Sudanese honey using Raman and Fourier transform infrared (FT-IR) spectroscopy, *Food Chem.*, **226** (2017), 202–211. http://doi.org/10.1016/j.foodchem.2017.01.024
2. Y. Y. Fu, J. Li, X. B. Li, S. Y. Wu, Damic event-triggered adaptive control for uncertain stochastic nonlinear systems, *Appl. Math. Comput.*, **444** (2023), 127800. https://doi.org/10.1016/j.amc.2022.127800
3. S. A. Collins, Lens-system diffraction integral written in terms of matrix optics, *Journal of the Optical Society of America*, **60** (1970), 1168–1177. https://doi.org/10.1364/JOSA.60.001168
4. M. Moshinsky, C. Quesne, Linear canonical transformations and their unitary representations, *J. Math. Phys.*, **12** (1971), 1772–1780. https://doi.org/10.1063/1.1665805
5. I. Daubechies, C. Heil, Ten lectures on wavelets, *Comput. Phys.*, **6** (1992), 697. https://doi.org/10.1063/1.4823127
6. H. M. Ozaktas, Z. Zalevsky, M. A. Kutay, *The fractional Fourier transform: with applications in optics and signal processing*, New York: Wiley, 1995.
7. D. Y. Wei, Y.-M. Li, The dual extensions of sampling and series expansion theorems for the linear canonical transform, *Optik*, **126** (2015), 5163–5167. https://doi.org/10.1016/j.ijleo.2015.09.226
8. J. J. Healy, M. A. Kutay, H. M. Ozaktas, J. T. Sheridan, *Linear canonical transforms: theory and applications*, New York: Springer, 2016. https://doi.org/10.1007/978-1-4939-3028-9
9. Y. Guo, B.-Z. Li, Bind image watermarking method based on linear canonical wavelet transform and qr decomposition, *IET Image Process.*, **10** (2016), 773–786. https://doi.org/10.1049/iet-ipr.2015.0818
10. M. Kundu, A. Prasad, Convolution, correlation and spectrum of functions associated with linear canonical transform, *Optik*, **249** (2022), 168256. https://doi.org/10.1016/j.ijleo.2021.168256
11. Z. C. Zhang, Jittered sampling in linear canonical domain, *IEEE Commun. Lett.*, **24** (2020), 1529–1533. https://doi.org/10.1109/LCOMM.2020.2988947
12. O. Ahmad, A. Achak, N. A. Sheikh, U. Warbhe, Uncertainty principles associated with multi-dimensional linear canonical transform, *Int. J. Geom. Methods M.*, **19** (2022), 2250029. https://doi.org/10.1142/S0219887822500293

13. A. Kumar, A. Prasad, Wigner-Ville distribution function in the framework of linear canoni-cal transform, *J. Pseudo-Differ. Oper. Appl.*, **13** (2022), 38. https://doi.org/10.1007/s11868-022-00471-w
14. D. Y. Wei, Y. J. Zhang, Y.-M. Li, Lnear canonical stockwell transform: theory and applications, *IEEE T. Signal Proces.*, **70** (2022), 1333–1347. https://doi.org/10.1109/TSP.2022.3152402
15. J. Y. Chen, Y. Zhang, B. Z. Li, Graph linear canonical transform: Definition, vertex-frequency analysis and filter design, *IEEE T. Signal Proces.*, **72** (2024), 5691–5707. https://doi.org/10.1109/TSP.2024.3507787
16. S.-C. Pei, J.-J. Ding, Closed-form discrete fractional and affine fourier transforms, *IEEE T. Signal Proces.*, **48** (2000), 1338–1353. https://doi.org/10.1109/78.839981
17. J. Zhao, R. Tao, Y. Wang, Smpling rate conversion for linear canonical transform, *Signal Process.*, **88** (2008), 2825–2832. https://doi.org/10.1016/j.sigpro.2008.06.008
18. A. Koc, H. M. Ozaktas, C. Candan, M. A. Kutay, Digital computation of linear canonical transforms, *IEEE T. Signal Proces.*, **56** (2008), 2383–2394. https://doi.org/10.1109/TSP.2007.912890
19. F. S. Oktem, H. M. Ozaktas, Exact relation between continuous and discrete linear canonical transforms, *IEEE Signal Proc. Let.*, **16** (2009), 727–730. https://doi.org/10.1109/LSP.2009.2023940
20. S.-C. Pei, S.-G. Huang, Fast discrete linear canonical transform based on CM-CC-CM decomposition and FFT, *IEEE T. Signal Proces.*, **64** (2016), 855–866. https://doi.org/10.1109/TSP.2015.2491891
21. B. M. Hennelly, J. T. Sheridan, Fast numerical algorithm for the linear canonical transform, *J. Opt. Soc. Am. A.*, **22** (2005), 928–937. https://doi.org/10.1364/JOSAA.22.000928
22. J. J. Healy, J. T. Sheridan, Sampling and discretization of the linear canonical transform, *Signal Process.*, **89** (2009), 641–648. https://doi.org/10.1016/j.sigpro.2008.10.011
23. J. J. Healy, J. T. Sheridan, Fast linear canonical transforms, *J. Opt. Soc. Am. A.*, **27** (2010), 21–30. https://doi.org/10.1364/JOSAA.27.000021
24. W.-L. Zhang, B.-Z. Li, Q.-Y. Cheng, A new discretization algorithm of linear canonical transform, *Procedia Engineering*, **29** (2012), 930–934. https://doi.org/10.1016/j.proeng.2012.01.066
25. S.-C. Pei, Y.-C. Lai, Discrete linear canonical transforms based on dilated hermite functions, *J. Opt. Soc. Am. A.*, **28** (2011), 1695–1708. https://doi.org/10.1364/JOSAA.28.001695
26. A. Koc, H. M. Ozaktas, Operator theory-based computation of linear canonical transforms, *Signal Process.*, **189** (2021), 108291. https://doi.org/10.1016/j.sigpro.2021.108291
27. D. Y. Wei, Y. Shen, Discrete complex linear canonical transform based on super-differential operators, *Optik*, **230** (2021), 166343. https://doi.org/10.1016/j.ijleo.2021.166343
28. A. Koc, H. M. Ozaktas, L. Hesselink, Fast and accurate computation of two-dimensional nonseparable quadratic-phase integrals, *J. Opt. Soc. Am. A.*, **27** (2010), 1288–1302. https://doi.org/10.1364/JOSAA.27.001288
29. D. Y. Wei, H. M. Hu, Sparse discrete linear canonical transform and its applications, *Signal Process.*, **183** (2021), 108046. https://doi.org/10.1016/j.sigpro.2021.108046

30. Y. N. Sun, W. C. Qian, Fast linear canonical transform for nonequispaced data, *Fractal Fract.*, **7** (2023), 353. https://doi.org/10.3390/fractalfract7050353

31. C. Anderson, M. D. Dahleh, Rapid computation of the discrete fourier transform, *SIAM J. Sci. Comput.*, **17** (1996), 913–919. https://doi.org/10.1137/0917059

32. S. Kunis, I. Melzer, Fast evaluation of real and complex exponential sums, *Electron. T. Numer. Ana.*, **46** (2016), 23–35.

AIMS Press